PROCEEDINGS OF THE ROYAL SOCIETY A MATHEMATICAL, PHYSICAL & ENGINEERING SCIENCES

Determination of an Organic Crystal Structure with the Aid of Topochemical and Related Considerations: Correlation of the Molecular and Crystal Structures of α-Benzylidene-γ-Butyrolactone and 2- Benzylidenecyclopentanone With Their Solid State Photoreactivity

S. K. Kearsley and G. R. Desiraju

Proc. R. Soc. Lond. A 1985 **397**, 157-181
doi: 10.1098/rspa.1985.0009

Proc. R. Soc. Lond. A **397**, 157–181 (1985)
Printed in Great Britain

Determination of an organic crystal structure with the aid of topochemical and related considerations: correlation of the molecular and crystal structures of α-benzylidene-γ-butyrolactone and 2-benzylidenecyclopentanone with their solid state photoreactivity

By S. K. Kearsley and G. R. Desiraju†
Department of Physical Chemistry, University of Cambridge, Lensfield Road, Cambridge CB2 1EP, U.K.

(*Communicated by J. M. Thomas, F.R.S. – Received 2 July* 1984)

[Plate 1]

The crystal structure of α-benzylidene-γ-butyrolactone **2**, can be determined with the aid of atom–atom pairwise energy evaluation procedures, because its (previously reported) solid state photoreactivity coupled with topochemical principles, greatly restricts the number of possible orientations of the molecule in the unit cell. Crystals of lactone **2** are monoclinic with space group $P2_1/n$ and with $Z = 4$, $a = 11.014(2)$, $b = 5.959(1)$, $c = 14.286(5)$, $\beta = 108.05(2)$. Refinement on 846 non-zero reflections led to an R (reliability) of 0.046. In contrast, the isoelectronic ketone 2-benzylidenecyclopentanone (**3**) is photostable, and crystallizes in the same space group with $Z = 4$, $a = 7.466(4)$, $b = 6.821(4)$, $c = 19.005(1)$, $\beta = 94.14(1)$. The structure of **3** was solved by direct methods and refined on 1037 non-zero reflections to an R of 0.036. The difference between the two structures can be rationalized in terms of intramolecular conformation and weak C–H···O hydrogen bonding.

Differences in the solid state photoreactivities of the two compounds can be related to the extent of orbital overlap between 'potentially reactive' double bonds on nearest neighbour molecules that are related by inversion. Compound **2** reacts in the solid state topochemically but not topotactically showing directional preference, while **3**, which has reduced orbital overlap, is photostable.

1. Introduction

The photodimerization of crystalline derivatives of 2-benzyl-5-benzylidenecyclopentanone, **1**, is in many ways a unique phenomenon in organic solid state chemistry. This 'diffusionless' reaction is topochemical wherein a direct correlation exists between the crystal structure of a reacting material and the molecular structure of the product (Cohen & Schmidt 1964; Schmidt 1971; Thomas 1974;

† Permanent address: School of Chemistry, University of Hyderabad, P.O. Central University, Hyderabad 500 134, India.

Thomas *et al.* 1977). Photo-irradiation of crystals of **1** rapidly leads to a quantitative yield of the head–tail anti-dimer in this manner (Thomas 1981), giving the spiro cyclobutane **1*a***. In addition, the reaction proceeds single-crystal to single-crystal without phase separation: when the product matrix can be crystallographically related to the reactant matrix then the reaction is said to be topotactic. This special feature of these photochemical solid state reactions lies in the fact that the reactant and product structures have unit cells that can be related to each other by some suitable crystallographic transformation. Also the product conformation is only marginally distorted from that of the reactants and the orientation of corresponding molecules within the crystals are similar. The conformational flexibility permitted in the carbon framework of the monomer allows the reactant to proceed smoothly to the product with minimal strain in the structure (Jones *et al.* 1980; Nakanishi *et al.* 1981). Topotaxy is an uncommon phenomenon and only a few other covalent bond-making processes in the organic solid state fall into this category; the polymerization of substituted diacetylenes (Wegner 1969, 1971), the early stages of diolefin (e.g. distyrylpyrazine) oligomerization (Nakanishi *et al.* 1980) and the thermal rearrangement of certain organic polyvalent iodine compounds (Gougoutas 1971, 1975). Small changes in the molecular structure can often lead to a considerable change in the crystal structure and concomitant loss of topotactic behaviour.

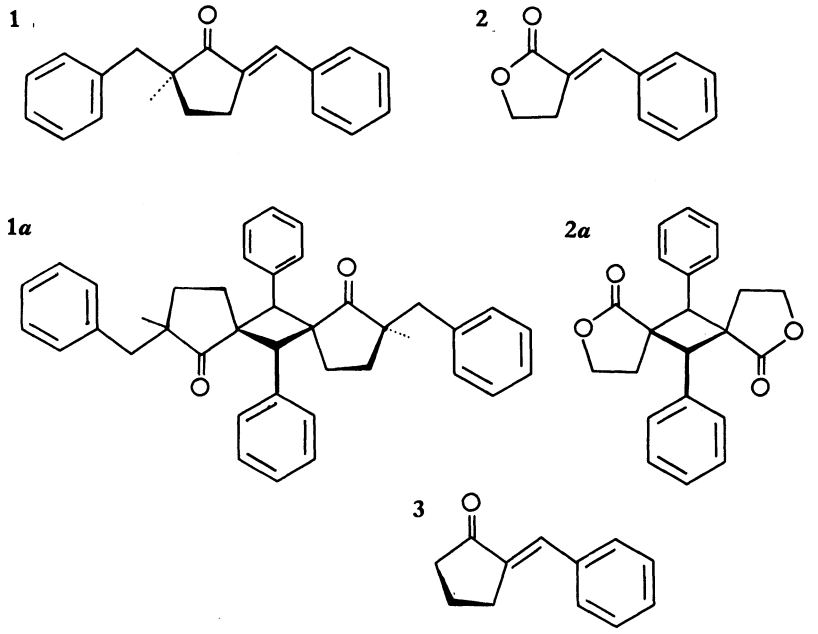

Scheme 1

This work was prompted by the recent observation that crystalline α-benzylidene-γ-butyrolactone **2**, a molecule similar to **1**, is converted quantitatively to the anti-dimer **2*a*** on irradiation with u.v. light (Kaupp *et al.* 1982). At the same time we found that the isoelectronic 2-benzylidenecyclopentanone, **3**, is photostable in

the solid state. Note that molecules **2** and **3** differ very slightly from one another, the methylene group being replaced by an oxygen atom, which has a closely similar volume. We therefore sought to answer the following questions; (i) is the dimerization of **2** topochemical and topotactic in a manner similar to **1**; (ii) assuming that the contrasting behaviour of **2** and **3** on irradiation is a consequence of topochemical factors, why are the two crystal structures different; (iii) are the differences between the crystal structures of **2** and **3** deep-seated or can they be systematically related to each other and to the structure of **1**?

In this work it was found necessary and expedient to solve the crystal structure of **2** by applying packing considerations and by using crystallochemical information because the structure could not be readily solved by direct methods. We have, therefore, used the atom–atom potential approach, which has previously been shown to be very successful in rationalizing close packing of organic molecules (Kitajgorodskij 1965; Williams & Starr 1977). For hydrocarbons in particular, these packing considerations have been used to solve the phase problem (Jones *et al.* 1978; Adams & Ramdas 1979), to describe the orientation of guest impurities in a host matrix (Ramdas 1979), to explain the phenomena of chiral turnover through a mechanism of cellular twinning (Ramdas *et al.* 1981) and non-topochemical reactions that take place preferentially at crystalline imperfections (Ramdas *et al.* 1977; Gramaccioli *et al.* 1980). It has been shown that compounds containing polar functional groups are more complicated to analyse because of the more dominant Coulombic terms in the potential and poorer heteroatom nonbonding potential parameters (Momany *et al.* 1974). Thus it was felt that an attempt to solve the crystal structure of polar lactone **2** by using packing considerations would be of interest. Furthermore, it was hoped to use some auxiliary chemical information as an alternative to an accurate knowledge of additional potential parameters.

2. Experimental section

2-*benzylidenecyclopentanone* (3)

This was prepared as a white solid (m.p. 67 °C) by the method of Birkofer *et al.* (1958, 1962). Well-formed prisms suitable for X-ray work were obtained from methanol. When solid **3** was irradiated under a mercury lamp for about 3 h at ambient temperatures (31 °C) small changes were observed in the i.r. spectrum. However, the olefin stretch at 1620 cm^{-1} and the carbonyl stretch at 1720 cm^{-1} were unchanged in position and relative intensity. The changes in the i.r. spectrum were ascribed to melting effects, because the material had become quite sticky. When irradiation was carried out at 0 °C for 24 h no changes were seen in the i.r. spectrum at all and the physical appearance of the compound was unchanged. Compound **3** is therefore photostable in the solid state.

α-*benzylidene*-γ-*butyrolactone* (2)

This was prepared by using procedures described by Reppe (1955) and easily recrystallized from ethanol to yield large colourless prisms (m.p. 115 °C) elongated along [010] and with main faces (101) and $(10\bar{1})$. When irradiated (in the form of

a KBr pellet) under a mercury lamp, photodimerization to cyclobutane **2a** was complete in about 2 h. When single crystals of **2** were irradiated for a few hours, the strain developed was sufficient to bend and finally to break them along (010) (figure 11*c*, plate 1). The rate of reaction for single crystals was seemingly much

TABLE 1. CRYSTAL DATA, INTENSITY DATA (ENRAF-NONIUS CAD4), COLLECTION PARAMETERS AND DETAILS OF REFINEMENT FOR COMPOUNDS **2** AND **3**

compound	ketone **3**	lactone **2**
a/Å†	7.466 (4)	11.014 (2)
b/Å	6.821 (4)	5.959 (1)
c/Å	19.005 (3)	14.286 (5)
β/deg	94.14 (1)	108.05 (2)
V/Å^3	965.3	891.5
space group	$P2_1/n$	$P2_1/n$
Z	4	4
D_c/g cm^{-3}	1.18	1.38
$F(000)$	368	368
μ/cm^{-1}	5.03	6.76
radiation Ni-filtered CuKα $\lambda = 1.54178$ Å		
crystal size/mm	$0.3 \times 0.25 \times 0.1$	$0.35 \times 0.15 \times 0.1$
$\theta_{min}/\theta_{max}$	3/65	3/70
scan mode	$\omega/2\theta$	
scan speed	variable	
scan width	$(0.85+0.15 \tan\theta)°$	
data measured	2234	2049
unique data	1708	1493
data observed	1037	846
significance test	$F_{obs} > 3\sigma F_{obs}$	$F_{obs} > 2\sigma F_{obs}$
refined parameters	170	159
number of suppressed observed reflections because of extinction	10	10‡
weighting scheme, g§	0.0006	0.01
final R‖	0.037	0.046
final R_w¶	0.037	0.047
goodness of fit, R_g††	0.042	0.057

† 1 Å = 10^{-10} m = 10^{-10} nm.

‡ Applied an empirical isotropic extinction parameter x where the calculated structure factors become: $F^* = F(1-0.0001\, xF^2/\sin\theta)$, x was refined to 0.058.

§ $w = k/[\sigma^2 F_{obs}^2 + gF_{obs}^2]$.

‖ $R = \Sigma[|F_{obs}|-|F_{calc}|]/\Sigma|F_{obs}|$.

¶ $R_w = \Sigma w^{\frac{1}{2}}[|F_{obs}|-|F_{calc}|]/\Sigma w^{\frac{1}{2}} F_{obs}$.

†† $R_g = (\Sigma w[|F_{obs}|-|F_{calc}|]^2/\Sigma wF_{obs}^2)^{\frac{1}{2}}$.

slower than in the case of **1** because the chipped crystal fragments gave zero-level Weissenberg photographs that were indistinguishable from those of the original unreacted crystal. The optical and Weissenberg photographs show that there was no phase separation; photoreaction was therefore a result of the original phase.

TABLE 2. FRACTIONAL COORDINATES (10^4) FOR LACTONE **2** WITH E.S.DS (ESTIMATED STANDARD DEVIATIONS) IN PARENTHESES (ISOTROPIC TEMPERATURE FACTORS FOR HYDROGENS ARE GIVEN)

	x/a	y/b	z/c	U
O-1	1325 (3)	−3495 (5)	−278 (2)	—
C-1	1666 (3)	−1770 (6)	165 (2)	—
O-2	2515 (2)	−435 (4)	−56 (2)	—
C-3	2748 (5)	1572 (8)	545 (3)	—
C-4	1962 (4)	1374 (7)	1244 (3)	—
C-5	1291 (3)	−812 (5)	985 (2)	—
C-6	471 (3)	−1927 (6)	1336 (2)	—
C-7	−39 (3)	−1390 (6)	2139 (2)	—
C-8	247 (4)	574 (7)	2709 (3)	—
C-9	−255 (4)	905 (8)	3469 (3)	—
C-10	−1053 (4)	−645 (8)	3676 (3)	—
C-11	−1361 (4)	−2575 (8)	3115 (3)	—
C-12	−863 (3)	−2930 (7)	2358 (3)	—
H-31	3648 (38)	1602 (67)	835 (27)	76 (13)
H-32	2472 (47)	2962 (99)	70 (33)	120 (19)
H-41	1375 (35)	2433 (69)	1138 (27)	65 (13)
H-42	2492 (36)	1458 (64)	1928 (26)	73 (12)
H-6	188 (29)	−3314 (56)	1032 (22)	40 (9)
H-8	859 (33)	1633 (64)	2556 (24)	62 (11)
H-9	−58 (32)	2306 (69)	3816 (25)	54 (10)
H-10	−1386 (30)	−418 (57)	4193 (24)	55 (10)
H-11	−1903 (33)	−3618 (62)	3249 (24)	55 (11)
H-12	−1056 (33)	−4336 (64)	1962 (26)	63 (11)

TABLE 3. FRACTIONAL ATOMIC COORDINATES (10^4) FOR KETONE **3** WITH E.S.DS IN PARENTHESES (ISOTROPIC TEMPERATURE FACTORS FOR HYDROGENS ARE GIVEN)

	x/a	y/b	z/c	U
C-1	2753 (3)	4780 (4)	5115 (1)	—
C-2	3021 (5)	2800 (4)	5463 (2)	—
C-3	2667 (5)	1328 (4)	4866 (2)	—
C-4	1345 (4)	2341 (4)	4336 (2)	—
C-5	1790 (3)	4473 (3)	4409 (1)	—
C-6	1573 (3)	5966 (4)	3957 (1)	—
C-7	737 (3)	5994 (3)	3235 (1)	—
C-8	−508 (4)	4608 (4)	2984 (1)	—
C-9	−1241 (4)	4668 (5)	2292 (1)	—
C-10	−761 (4)	6133 (5)	1849 (1)	—
C-11	426 (4)	7539 (5)	2089 (1)	—
C-12	1167 (4)	7489 (4)	2782 (1)	—
O-1	3235 (3)	6340 (3)	5365 (1)	—
H-21	2198 (34)	2796 (39)	5812 (14)	76 (9)
H-22	4236 (35)	2709 (37)	5707 (12)	73 (9)
H-31	3929 (49)	1157 (50)	4656 (17)	94 (13)
H-32	2152 (37)	112 (44)	5032 (14)	83 (9)
H-41	52 (33)	2043 (33)	4425 (11)	58 (7)
H-42	1442 (34)	1875 (37)	3842 (13)	80 (9)
H-6	2088 (28)	7274 (30)	4126 (10)	47 (6)
H-8	−877 (31)	3554 (34)	3297 (12)	69 (8)
H-9	−2096 (37)	3685 (39)	2120 (14)	96 (10)
H-10	−1269 (32)	6180 (33)	1333 (13)	73 (8)
H-11	692 (35)	8653 (38)	1835 (13)	81 (9)
H-12	2013 (30)	8470 (32)	2944 (11)	61 (8)

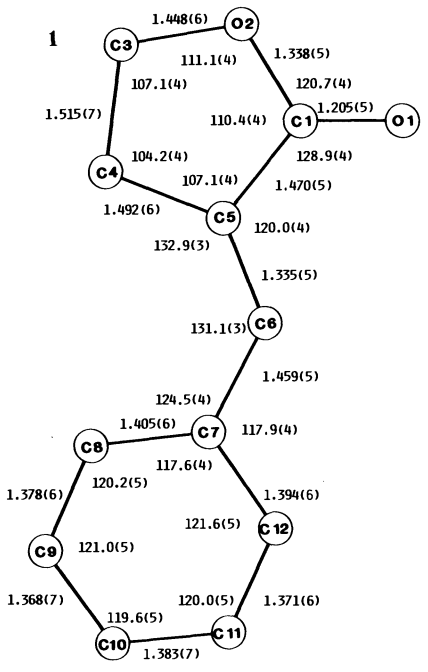

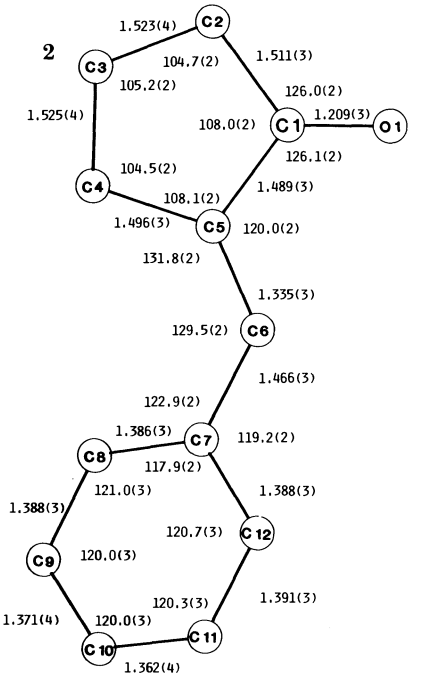

FIGURE 1. Atom numbering, bond lengths (ångströms) and angles (degrees) for lactone **2**.

FIGURE 2. Atom numbering, bond lengths (ångströms) and angles (degrees) for ketone **3**.

X-ray structure determination of lactone **2** *and ketone* **3**

Most of the details of the unit cell, data collection procedures and refinement are given in table 1. The structure of **3** was solved without difficulty by direct methods. The structure of **2** could not be solved with the routine application of the programs MULTAN 80 (Germain *et al.* 1971) or SHELX-76 (Sheldrick 1976), but a solution was obtained by using 'real space' packing considerations as described in the following section. For both structures, the positions of the hydrogen atoms were obtained from difference maps, these positions and isotropic thermal parameters being allowed to vary in the conventional full matrix least squares procedure (SHELX-76), which concluded satisfactorily at R-values of 0.042 and 0.037 for structures **2** and **3** respectively. Therefore the intra- and intermolecular bond lengths and angles involving the hydrogen atoms are reasonably accurate. Coordinates are given in tables 2 and 3; atom numbering, bond lengths and angles are displayed in figures 1 and 2.

3. STRUCTURE DETERMINATION OF LACTONE

The principal difficulty encountered when using conventional methods of structure solution for **2** lies in the presence of a very intense reflection (202) where $F(202) = 0.42F(000)$. Intensities of this magnitude are always a problem in direct methods and yet their down-weighting or even complete removal may not always

lead to the correct solution. The recent structure determination of 3,4-dimethoxycinnamic acid (Desiraju *et al.* 1984) illustrates some of the problems encountered when a single reflection is very intense.

We worked on the plausible assumption that the solid state photodimerization of **2** is topochemical. This is reasonable because there is much evidence in the literature for such $\pi 2s + \pi 2s$ solid state reactions to be so (Cohen & Schmidt 1964 and succeeding papers; Paul & Curtin 1973). Compound **1**, which offers the most obvious comparison, is probably one of the more well known examples (Thomas 1981). Furthermore, from the structure assigned by Kaupp *et al.* (1982) to the solid state photoproduct from **2**, and by analogy with **1**, it can be assumed that the dimerization reaction of **2** is topochemical and that the incipient dimer (i.d.) lies across a centre of inversion; thus the potentially reactive double bonds must be approximately 4 Å from one another. (Note that the i.d. term is also applied to potentially reactive molecules of **3** and in this context signifies only the inversion-related molecular pair.)

The procedure then adopted involved two broad stages; (i) analysis of the mutual disposition of monomers within the isolated i.d. configuration, and (ii) optimization of the orientation of this monomer pair in the cell subject to crystallographic constraints (crystal symmetry, cell dimensions). Calculations used the PCK6 version of Williams' program (1972) where only the dispersive and repulsion energy terms were monitored as the superposition of pairwise atom–atom potentials; the familiar Buckingham model was used:

$$U = \tfrac{1}{2}\sum (B_{\alpha\beta} \exp(-C_{\alpha\beta} r_{ij}) - A_{\alpha\beta}/r_{ij}^6).$$

In the first stage, analysis involves the investigation of the interaction energy of all possible configurations of the isolated incipient dimer pair. The interaction energy can be expressed in the form of contour maps, which are slices through the explored energy surface parallel to the plane defined by the axis of maximal moment of inertia.

Figure 3 shows an isolated pair of molecules with variation in the z-direction

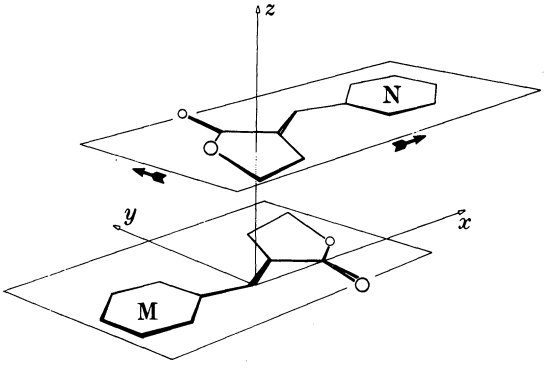

FIGURE 3. Diagram showing the frame of reference used in constructing the energy surface associated with an isolated pair of molecules related by inversion (see text for details).

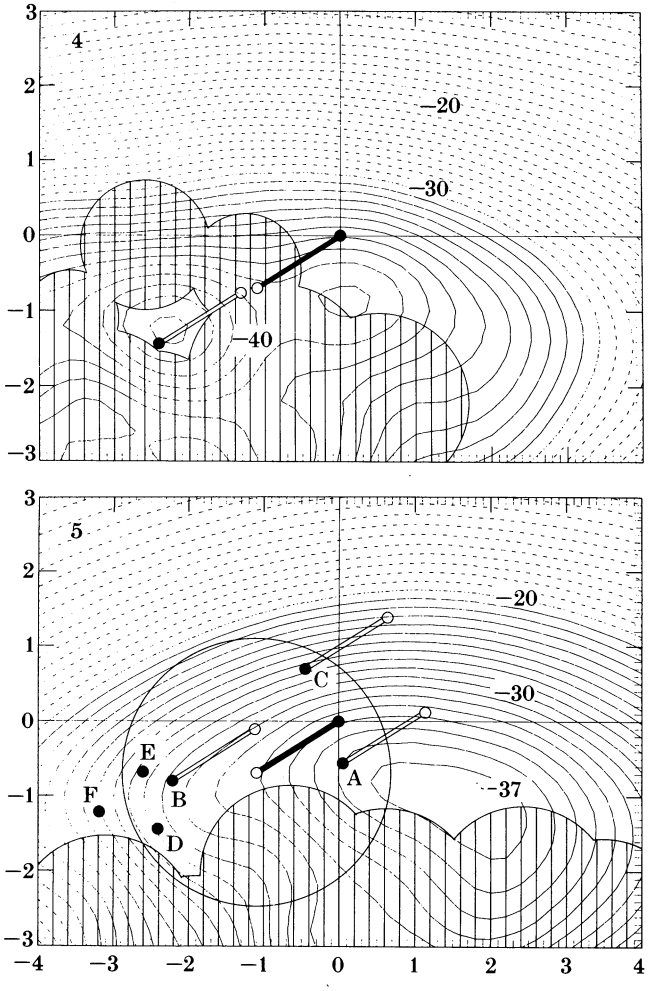

FIGURE 4. Contour map for compound **1**. The axes are in units of ångströms with contours at 1 kJ mol^{-1} intervals. The shaded area denotes unfavourable short contacts arising from methylene hydrogens with atoms on the neighbouring molecule. Drawn on the map are the reactive double bonds in their crystallographic configurations; the shaded bond belongs to the stationary molecule. The p.a.p. (black atom) indicates that this configuration is at a minimum of −43 kJ mol^{-1}. Maps similar to this for other derivatives of **1** also show that the crystallographic configuration corresponds to the minima found on the energy surfaces.

FIGURE 5. Contour map for compound **2** based on the partial atomic framework of **1**. The plane separation is set at 3.8 Å. General details are the same as for figure 4. The radius of the circle is defined as $(4.2^2–3.8^2)^{\frac{1}{2}}$ and the centre is placed on the C-5 atom of the stationary molecule, thus if the p.a.p. (anti-parallel atom C-6) lies within the circle the double bonds will be at a distance less than 4.2 Å and likely to undergo a topochemical reaction. A, B and C show the positions of the three trial i.ds. D, E and F show the crystallographic orientations of **1**, **2** and **3** respectively (these correspond to the drawings of the i.ds in figure 6). Note although F is outside the circle and the double bonds for **3** are at a separation of 4.1 Å it must be remembered that this is not the crystallographic plane separation and F would appear in a circle drawn on a map derived by using the atomic coordinates of **3**.

defining the separation of the molecular planes. Molecule M is fixed whilst molecule N is translated in the x–y plane so that the inversion symmetry and interplanar separation between M and N are maintained. Thus a unique contour map can be defined. To calculate the potential associated with a particular molecular configuration, it is convenient to designate a reference point in the molecules. For molecule M, this point is always on the origin, and for molecule N its position defines the x–y translation on the map while the contour height gives the interaction energy of the i.d. pair. For all our maps the 'potential association point' (p.a.p.) is conveniently chosen as the C-6 atom and thus the origin for each map corresponds to the orientation of the two molecules where the C-6 atoms in each unit are superimposed in the z-direction. Atoms C-1 and C-6 of molecule M define the x-axis and the line between these atoms in molecule N must remain parallel to the x-axis to maintain the symmetry operation. Minima on the contour map refer to the best energetic orientations of the isolated molecular pair, M and N. This minimum is subject to the exclusion of individual repulsive short contacts, because in general this leads to a dynamically unstable structure (Gramaccioli *et al.* 1980). It was expected that an analysis of this type would be appropriate for the crystal structure of **2**. This is because it is found, without exception, for the eight derivatives of **1** (where the centrosymmetric pair motif exists in the crystal structure), that the minimum energy configuration of the isolated pair corresponds to that actually found (to within 2 kJ mol^{-1}) in the crystal structure of the infinite assembly of molecules. Figures 4 and 5 show the maps for **1** and **2** respectively.

The second stage concerns a selective use of the packing program. This program minimizes the lattice energy, a function of at least twelve variables (Williams 1969, 1972), of which six (unit cell parameters) can be held constant. The remaining six refer to the orientation and position of the molecule in the cell and have to be determined.

The energy parameters A, B and C (table 4) are those of Williams & Starr (1977) and Cox *et al.* (1981), and are used in computing interactions less than 6.5 Å; the remainder of the lattice sum was evaluated by a convergence approximation (Williams 1971).

TABLE 4. POTENTIAL PARAMETERS†

interaction	A/(kJ mol^{-1} Å^6)	B/(kJ mol^{-1})	C/Å^{-1}	minimum/Å
C—C	2414.00	367250	3.60	3.90
H—H	136.00	11677	3.74	3.30
O—O	1123.59	230064	3.96	3.40

† The geometric mean combining law was assumed for A and B, and an arithmetic mean for C, to generate cross-atom type interactions. The potential minima for C—H, C—O, H—O interactions are 3.60, 3.64, 3.36 Å respectively.

The position of the molecule in the cell could be tied to the rotation variables as the i.d. must be placed on a centre of symmetry (topochemical principle); thus the second stage only involved the optimization of the i.d. with respect to the Euler angles. This was done in the hope that there would be now a better chance of attaining a global minimum for the structure.

Before the i.d. geometry can be optimized it is necessary to have some knowledge of the conformation of the five-membered ring in **2**. Fortunately, there exists a substantial body of crystal structure data on related derivatives of **1** (Nakanishi *et al.* 1981 and references cited therein; Kearsley 1983).

TABLE 5. MOLECULAR DESCRIPTION OF CONTACTS FOR LAMINAR SHAPED MOLECULES

description of contacts	motifs formed	identified by	strength of interaction	contribution to lattice energy
plane-to-plane	columns or inversion dimers	C···C	very strong	large
plane-to-edge	herring-bone	C···H	strong	very large
edge-to-edge	interaction between major motifs	H···H	weak	small

For almost all photoreactive modifications of **1**, the benzylidenecyclopentanone conformations are similar and much more planar than the conformation of the non-reactive ketone **3**. A detailed description of the structure of **3** is given later, but at this stage it is sufficient to state that because of its non-planar configuration it is unlikely to have good plane-to-plane contacts for the inversion pair (see table 5 for an explanation of contact types). On the other hand the potentially reactive double bonds in **2** are in the middle of the carbon framework and for the compound to photoreact it must be more planar than **3**. For these reasons, the relevant coordinates from **1** were used (where the benzylidenecyclopentanone fragment is almost planar), with the superfluous atoms removed or exchanged so as to obtain the **2** framework. The plane separation was set at 3.8 Å and produced the results shown in figure 5. It was found in general that the surface does not alter a great deal for plane separations between 3.6 and 4.0 Å.

Three dimer configurations that were sufficiently different were initially chosen. All these satisfied the following four criteria;

(i) the p.a.p. must be within 10 kJ mol^{-1} of the minimum;

(ii) atoms were staggered as much as possible because the molecules must have some displacement from total overlap. Total overlap would result in too many weak H···H interactions and problems in close-packing for the coordinating molecules;

(iii) the p.a.p. must be in the circle that defines the limit of reactivity;

(iv) the lactone hydrogens should not interfere with the planar section of the neighbouring molecule. Regions in the map excluded for this reason are shown by the shaded lines.

Each of the three positions for the i.d. had the following special features;

(*a*) although fairly well overlapped, it is the nearest to the energy minimum of the map and displays excellent carbonyl–benzene ring interactions. This type of configuration between such groups is thought to have some influence on the packing, though (with respect to geometry and nonbonding forces) there is no extra reason why this configuration should be favourable;

(*b*) displacement was along the length of the molecule;
(*c*) displacement was along the width of the molecule.
The configurations are shown in figure 6 (*a*, *b*, *c*).

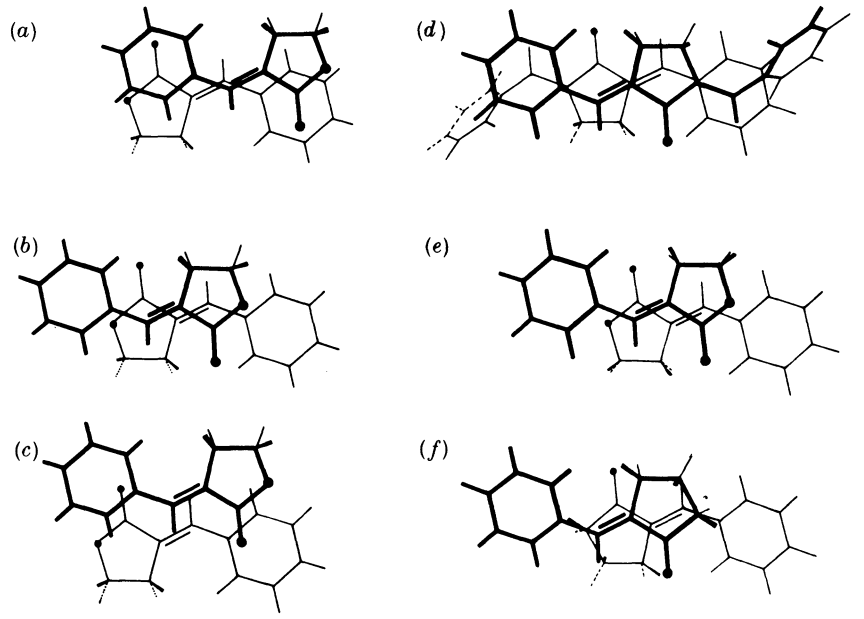

FIGURE 6. Orientations of the molecules described in figures 4 and 5. *a*, *b* and *c* are trial orientations for **2**; *d*, *e* and *f* are crystallographic orientations of the i.d. for **1**, **2** and **3** respectively.

To implement the packing program, the i.d. defined above was generated and the centroid of the dimer placed at the inversion centre on the origin. The initial starting position of the molecule was therefore not arbitrary nor need it be since the topochemical properties restrict the possible interaction configurations of the inversion related pair. Also, by matching the molecular dimensions (*ca.* 11 Å × 6 Å × 4 Å) with the unit cell dimensions one can conclude that only certain orientations with respect to the axes are possible for the molecule. More specifically, the small value of *b* restricts the possible molecular orientations. From observation of the crystal during irradiation, the direction of reaction and crystal fracture along [010] would seem to indicate that the molecular planes are parallel or nearly parallel to [010].

The first optimization involved only the three Euler angles. Configuration *a* led to no reasonable structure as there were too many bad contacts along [100] (figure 7*a*). Configuration *b* was far more promising, but when its orientation was allowed to optimize the i.d. remained virtually stationary and did not tilt even slightly from [010]. The unfavourable contacts were now between molecules related by translation along the [010] direction implying that a tilt was indeed necessary. Although the molecules have their long axes nearly parallel to [100], they are not exactly so, because reflections like (212) and (414) have substantial

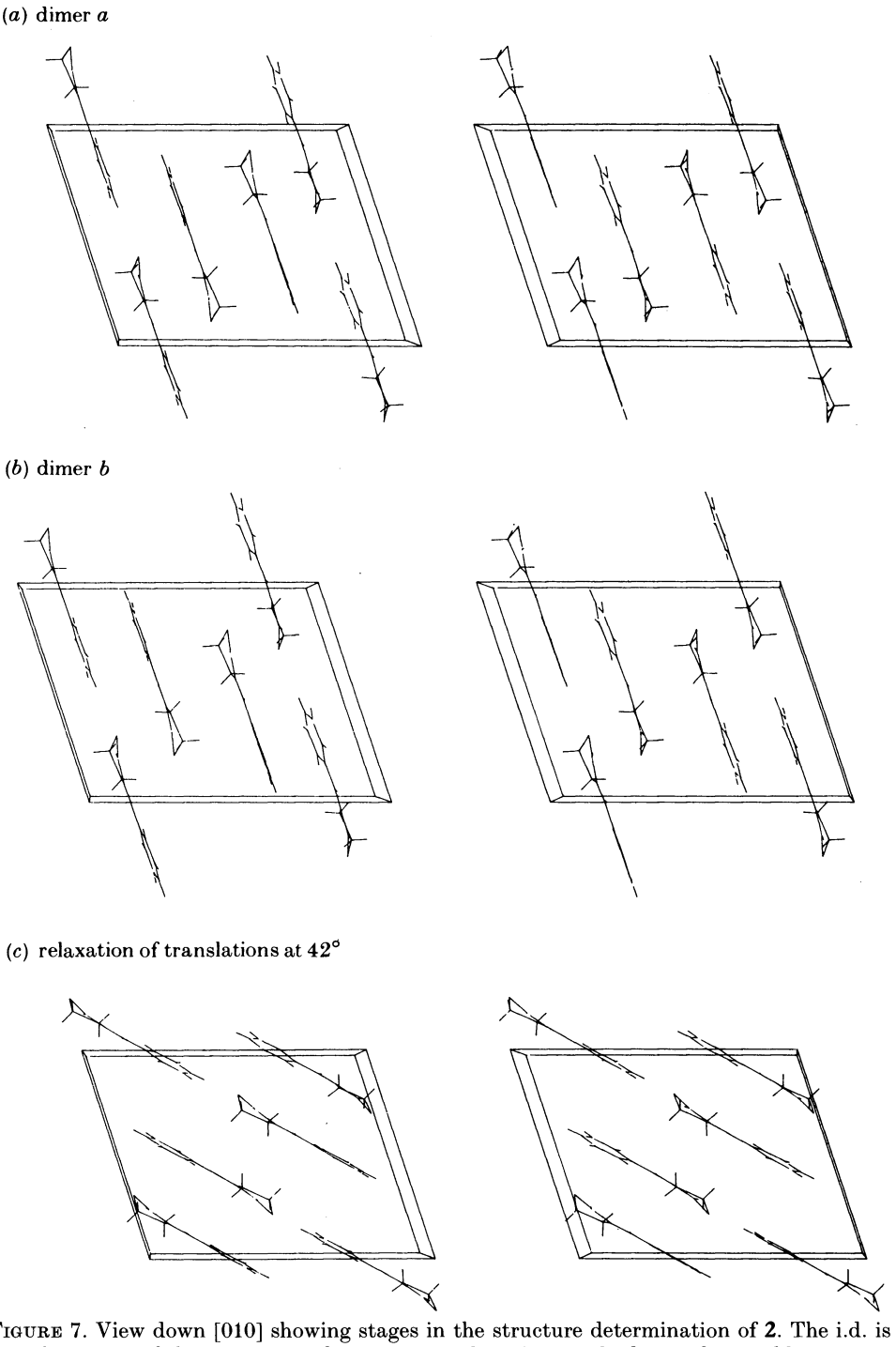

FIGURE 7. View down [010] showing stages in the structure determination of **2**. The i.d. is at the centre of the cell. (*a*) configuration *a*; relaxation resulted in unfavourable contacts in [010] along the length of the molecule. (*b*) configuration *b*; after relaxation the molecule remained at this initial starting orientation. (*c*) By using configuration *b* and manually

(*d*) relaxation of Euler angles

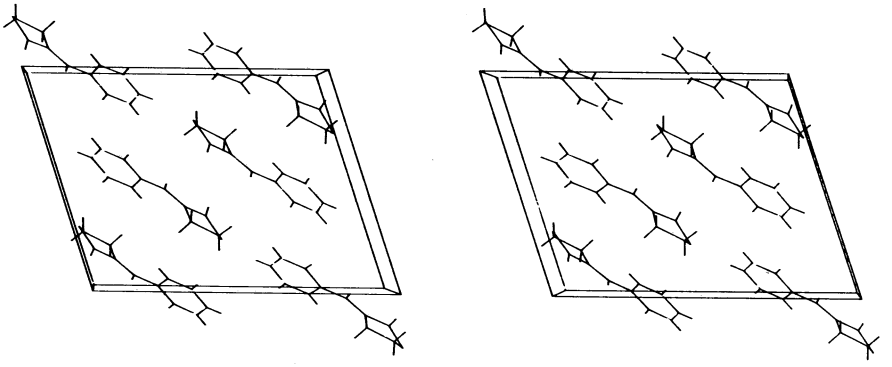

(*e*) global minimum

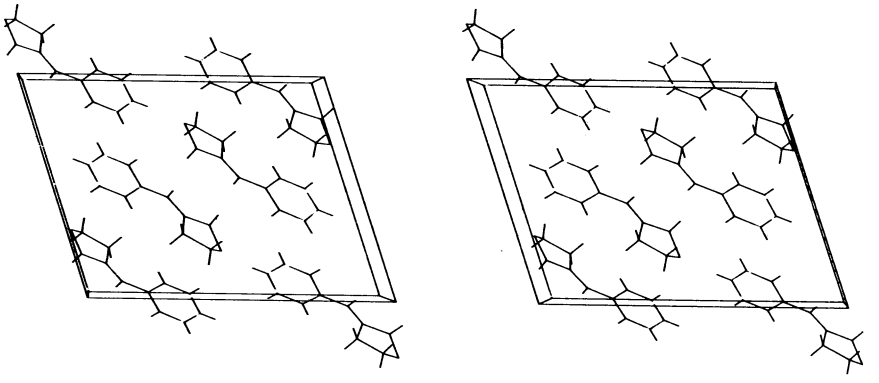

(*f*) refined structure

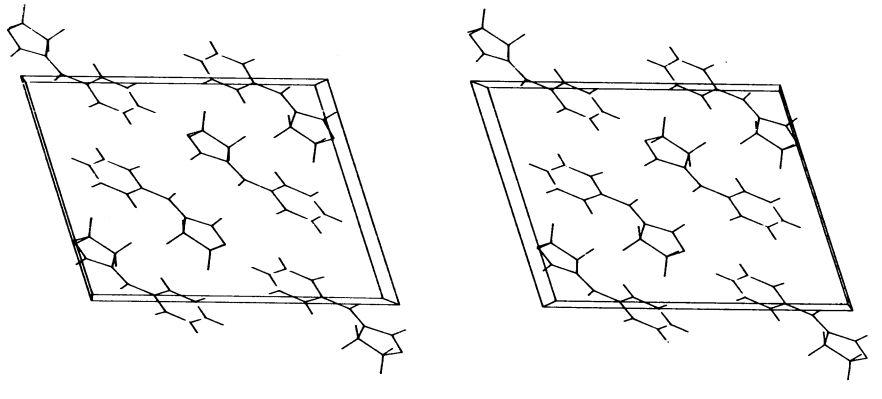

orientating the plane normal of the molecule to coincide with (202), c is obtained. The translation variables were relaxed to slightly adjust the i.d. configuration. (*d*) The Euler angles were allowed to relax for the i.d. (*e*) The monomer was allowed to relax freely and locked into the global minimum. (*f*) The refined crystal structure for comparison.

diffraction amplitudes. When subjected to clockwise rotation about [010] before optimization, the dimer always returned to its original starting orientation, where the length was aligned along [100]. However, rotations from the starting position anticlockwise about [010] towards the origin seemed to be far better, implying that the preferred orientation of the length of the molecule would be along [10$\bar{1}$]. It was noted that the diagonal [101] was of length 16 Å, corresponding to four stacked molecules in this direction. This observation concurs well with the large value of $F(202)$. The return of the i.d. to the original starting position probably underlines the fact that the restriction of the geometry of the monomer units was too stringent and produced too many 'locking' interactions. Local minima such as these are not possible in the crystal structures of organic molecular solids, but these dynamically unstable structures can be realized for amorphous materials as exemplified by the work of Eiermann *et al.* (1983) on films of tetracene and pentacene. Several other approaches were tried. For example, random orientations of the monomer, not too surprisingly, did not lead to the correct structure. The cell of molecule **3** was 'flattened' so that the benzene and cyclopentanone rings were coplanar and the C-2 methylene group was replaced by oxygen; the lactone cell was subsequently fitted around this pre-orientated molecule in the hope that the molecular positions were similar within the cell, but this also produced no results.

We noted next that an inspection of the structure amplitudes showed a group of ($h0l$) reflections that have substantial intensity. This observation points to the fact that the (010) planes are especially densely packed. It is no surprise that the photodimerization reaction spreads rapidly in this plane, leading to crystal fracture perpendicular to [010]. Because the most intense reflection was (202), it was decided to align the length of the molecule parallel to the plane causing this reflection by rotating around [010] (entailing a movement of 42° anticlockwise; see figure 7*c*). The optimization proceeded in two stages. First, the i.d. configuration was optimized at this fixed orientation, by varying the translation and rotation variables sequentially; this resulted in a shift in position of 0.25 Å (the final result of these operations is shown in figure 7*d*). Second, the monomer was totally released and Euler angles and translations were allowed to vary. The structure moved into the global minimum immediately giving a final lattice energy of -83 kJ mol^{-1}, comparable with that of **3** (-83 kJ mol^{-1}).

Figure 7(*a–f*) gives a pictorial representation of the various states of the structure determination. For the final orientation, the plane normal moved away from (010) by 23°, as perhaps indicated by the moderately strong reflections (212) and (414). The initial orientation regarding the projection of the plane normal on (010) was hardly changed.

When the coordinates obtained from the packing program were fed into the least squares procedure (Sheldrick 1976), the starting R was 0.40. Refinement was completely satisfactory and converged at an R of 0.042 with all atoms included (C and 0 atoms having anisotropic thermal parameters). The final orientation of the molecular plane was (423).

4. Comparison of lactone and ketone crystal structures

The crystal structures and packing arrangements of lactone **2** and the isoelectronic ketone **3** reveal many subtle similarities as well as important differences. The replacement of the lactone oxygen by a methylene group is hardly expected to make a difference in the general shape and volume of the molecules. The volumes are 167 and 175 Å^3 for **2** and **3** respectively. In both compounds, an important dipole interaction is the antiparallel arrangement of carbonyl groups on near neighbour molecules. This interaction can be conveniently optimized by the location of an inversion centre between pairs of such molecules. Thus, similar volume, shape and symmetry criteria lead to the same centrosymmetric space group $P2_1/n$ and comparable unit cell dimensions.

There are nevertheless striking differences in the two structures, and these are most obviously manifested in the solid state photoreactivities. Another seemingly minor yet physically significant distinction between the two compounds lies in their melting points. Lactone **2** has a melting point of 115 °C while ketone **3** melts almost 50° lower (67 °C), a fairly substantial difference. Considering that **1** has a melting point of 121 °C, it would seem that **3** has a 'normal' melting point while that of **2** is anomalously high. These effects are reinforced in the appreciable differences in density, 1.38 and 1.18 g cm^{-3} for **2** and **3** respectively. All this indicates that the polar lactone can adopt a structure with a more favourable lattice energy than the ketone.

(*a*) *The intramolecular structures*

In both compounds the bond lengths and angles are normal and are displayed in figures 1 and 2. Almost all the features of the structures and through them, their physical and solid state chemical properties, can be directly or indirectly traced to the high degree of planarity of the molecule **2** and lack thereof in **3**. This difference in planarity can be related to the replacement of the —CH_2— group in **3** by the —O— atom in **2**. The O-2 oxygen in **2** (the ether linkage in the lactone) is partly conjugated with the α, β-unsaturated carbonyl system (see figures 1 and 2 for comparison of bond lengths for atoms attached to O-2 in **2** and C-2 in **3**). Also, the absence of the methylene hydrogens (H-21 and H-22 in ketone **3**) relieves, to some extent, the eclipsing interactions that are present in **3**. This means that in **2** the five-membered ring can be accurately planar. Indeed, the entire molecule is planar with a maximum deviation of the non-hydrogen atoms from the mean molecular plane of 0.05 Å. The conformation of the cyclopentanone fragment in **3**, however, resembles those of the derivatives of **1**. The C-3 atom deviates the most (0.5 Å) from the mean plane defined by C-1, C-2, C-4 and C-5 thus minimizing steric strain between cyclopentane hydrogens (Kearsley 1983).

In **3**, the benzene ring is rotated about C-6–C-7 so that the torsion angle (C-5···C-6–C-7···C-8) is 23°, reducing the conjugation energy. In comparison, the entire molecule of **2** tends to be planar because of the planarity of the five-membered (lactone) ring, because this affords the possibility of more compact packing (hence a greater density and m.p.). For both **2** and **3**, the angle C-5–C-6–C-7 is within a degree of 131° and nonbonded distances involving H-41, H-42 and H-8 are very similar. The relatively puckered five-membered ring of **3** leads to a more irregularly

shaped molecule, because there is no particular advantage in the phenyl ring being coplanar with the mean plane of C-1, C-4, C-5 and C-6. It may also be noted that for photostable derivatives of **1** where the major motif is generated by two glide planes, and characterized by predominantly plane-to-edge contacts, the deviation from 0° of the corresponding torsion angle is much greater than for the more planar reactive derivatives (Kearsley 1983). Applying standard molecular mechanics programs, the conformation of each structure was relaxed using the crystallographic coordinates as a start configuration. The lactone remained much the same, but the ketone relaxed to a planar π-conformation. The refinement of bond compression terms made the difference in other internal energy terms (for example van der Waals and torsion forces) less interpretable. We suggest that the torsion angles between the 5- and 6-membered rings in the two structures are decided on the basis of intermolecular forces, rather than on relief of steric strain.

(*b*) *The incipient dimer configurations*

For organic molecular solids in general, plane-to-plane contacts contribute substantially to the lattice energy and entail either inversion or translation symmetry operations. We have referred to the fact that for many structures which incorporate plane-to-plane or stacking motifs it is found that the most stable configuration for the isolated pair of symmetry related molecules, as obtained from the contour maps, corresponds closely to that found in the actual crystal structure. In other words, since the nonbonding interactions for the pair of molecules are so strong, the structure of the motifs are, to a first approximation, only slightly dependent on the nature of the packing of the surrounding molecules. Thus the properties involving just the structural motif can be rationalized without a full knowledge of the entire crystal structure. For derivatives of **1** displaying such a motif, the above is certainly true in the sense that the i.d. pair lies within less than 2 kJ mol^{-1} from the minimum of the contour map (figure 4). Information obtained from the maps using the refined coordinates of **2** and **3** show that the isolated i.ds are displaced from the minimum by about 7–8 kJ mol^{-1}. The maps are very similar in profile to the one shown in figure 5. Although the minima for both maps (near position A, on figure 5) do not correspond exactly to the i.d. geometry in the actual structures, (seemingly contradicting the above discussion of the i.d. geometry), this is not unusual and it will be seen that the loss of about 7–8 kJ mol^{-1} is compensated by other favourable packing interactions.

The displacement of molecules within the i.ds is such that the five-membered rings overlap to a greater extent along the length of the molecule (figure 6). The greater plane separation in **3** (3.58 Å in the plane defined by the olefin and carbonyl only; if a plane were selected through all the non-hydrogen atoms a 3.8 Å separation would result) as opposed to **2** (3.39 Å) is a consequence of the nonplanar five-membered ring and the steric interactions of the C-2 hydrogen atoms in the former. The plane separation distance in **2** is exceptionally small. For these plane-to-plane geometries, the i.ds for **2** and **3** contribute predominantly to the total lattice energy (40 and 30% respectively). The subtle differences in plane separation and the slightly more displaced inversion-related pair of **3** compared to **2** (cf. figure 6 *e*,*f*) allows the benzene ring in **3** the freedom to pack independently

of the adjacent cyclopentanone in the opposing molecule; i.e. it can rotate by 23° without causing bad interactions within the i.d.

Several of the properties of **2** and **3** can be explained when they are compared with the i.d. configuration of **1**. Although the orientation of the (five-membered ring)–benzylidene fragments in the i.ds differ little in **1**, **2** and **3**, the minimum for **1** has moved to position D on the map, figures 4 and 5. The extra interactions that move the minimum for **1** to this point are derived from the benzyl group, which has conformational freedom about two bonds. The configuration of the i.d. can be therefore optimized with respect to these subrotations and this has great bearing on the topotactic photodimerization of **1**, and lack thererof in **2**.

(*c*) *Solid state reactivity*

The distances between the centres of the olefinic (incipient cyclobutane) bonds of the inversion related molecules in the i.d. are 3.67 and 4.14 Å for **2** and **3** respectively. It is generally accepted that the threshold value for the double bond separation for solid state reactivity of this type is around 4.2 Å (Schmidt 1971) and by this token both compounds ought to be photoreactive in the crystal. The i.d. geometry does not differ greatly for the two compounds, and yet while **2** reacts in the solid state, **3** does not. This dichotomy is resolved when orbital overlap rather than centre-to-centre double bond separation is considered.

Figure 8 shows projections of the double bond pair configurations; for both compounds the double bond centres of the inversion related molecules lie within the arcs and circles defining the limit of 4.2 Å. One should note, however, that the lateral shift (point E to F on the contour map, figure 5) is about 0.75 Å more for the ketone than for the lactone. This, in effect, implies greatly reduced π-orbital overlap for molecules in the i.d. for **3** compared to **2**. The difference in the orbital overlap can be clearly seen in figure 8 and it is this reduced overlap in **3** that accounts for its solid state photostability. A crude quantification of the potential orbital overlap can be taken by measuring the distances between the hypothetical lobes of the reacting atomic orbitals; in this case, the apices of the p-orbital lobes perpendicular to the plane of conjugation for the atoms involved in the 2+2 cycloaddition. The coordinates of point T in figure 8 are constructed by taking the plane normal through the reacting carbon atom and the adjacent bonding atoms; this vector is given a magnitude of 1.8 Å (the van der Waals radius for carbon).

The distance T to T' gives a measure of the lobe-to-lobe overlap between reacting atoms, and the smaller this distance, the better the overlap. Table 6 shows how this measure of overlap correlates with the actual solid state reactivity of the compounds. For example, in the case of the lactone **2**, ketone **3** and compound **1**, the overlap for **3** is markedly reduced. To corroborate this, the non-parallel double bonds in dibenzylidenecyclopentanone (Kaupp & Zimmermann 1981; Theocharis *et al.* 1984) are expected to give both mirror and rotationally symmetric dimers whereas octatetraene (Drenth & Wiebenga 1955) shows very little overlap and is thus unreactive. Also, in the case of 1,1′-trimethylenebisthymine (Frank & Paul 1973), the preference for the intermolecular over intramolecular reaction in the solid state becomes more apparent. In general, one cannot expect a 100% correlation between the disposition of point atoms in the solid state and the

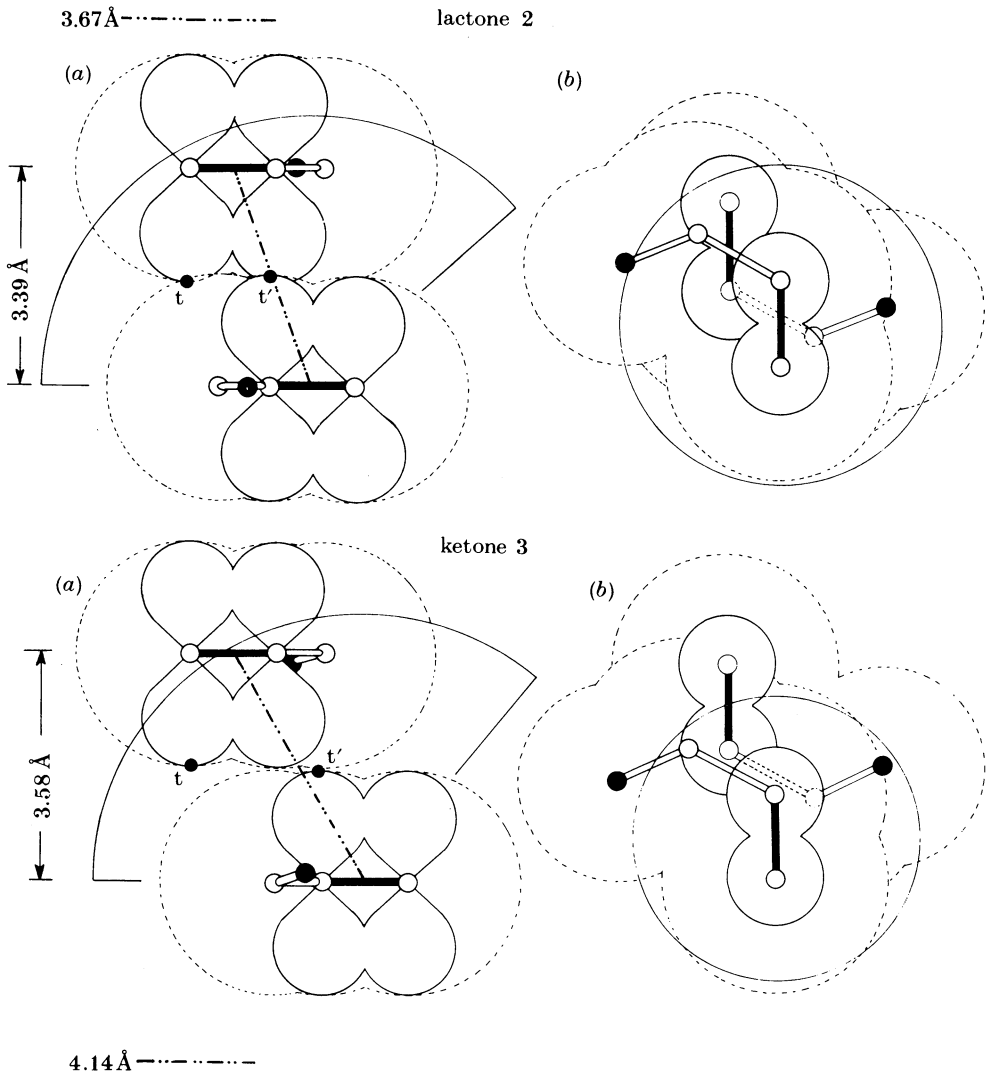

FIGURE 8. Schematic depiction of the orbital overlap for both compounds. These diagrams are constructed from the crystal data. The shaded bonds are the olefinic functionals and the shaded atoms are oxygen. Two projections are shown; (*a*) a view perpendicular to the length of the double bond and within the plane of conjugation; (*b*) looking upon the plane of conjugation and hence along the direction of the reacting p_z orbital.

For (*a*), the arc (more properly a spherical shell), shows the 4.2 Å boundary. This is drawn from the centre of one double bond with the lower double bond taken as a reference point. The circles drawn in (*b*) are derived from the plane cutting the spherical shell; thus the radius is a function of the plane separation and shows the 4.2 Å limit for this separation. Also marked on the diagrams are the perpendicular separations of the double bonds and the bond-centre to bond-centre distance. The dashed line is the van der Waals envelope drawn about the molecular fragment (1.8 and 1.54 Å for carbon and oxygen).

TABLE 6. GEOMETRIC INFORMATION PERTAINING TO PHOTOREACTIVITY (SEE TEXT)

	separation	distance	lobe 1	lobe 2	(lobe 1 + lobe 2)	
compound	Å†	Å‡	Å§	Å§	Å	reactivity‖
lactone	3.39	3.67	1.47	1.47	2.94	yes
ketone	3.58	4.10	2.15	2.15	4.30	no
compound 1	3.82	4.12	1.57	1.57	3.14	yes
octatetraene¶		3.89	3.20	3.39	6.59	no
		4.10	3.00	2.69	5.69	no
dibenzylidenecyclopentanone						
mirror	3.60	3.67	0.95	0.92	1.87	yes
rotation	3.60	3.67	0.48	2.06	2.54	yes
1,1′-trimethylenebisthymine						
intra-	3.19	3.50	1.52	1.65	3.17	no
inter-	3.63	3.69	0.86	0.82	1.68	yes

† Separation refers to the plane separation.
‡ Distance refers to the bond-centre to bond-centre.
§ Lobe 1 and lobe 2 are the distances T–T'' for the two lobe pairs.
‖ Reactivity does not imply that the reaction is topochemical.
¶ A separation for the two possible bond formations in octatetraene are not given as the double bonds are too askew.

reactivity, which is predominantly an electronic phenomenon; and thus such rationalizations, based upon geometric information, can serve little predictive value.

The crystal structure of **2** shows that the production of the anti-dimer on solid state irradiation as reported by Kaupp *et al.* (1982) must be the result of a topochemical reaction. Our experiments with single crystals demonstrate that the reaction is not topotactic in comparison with **1**. As outlined above this result is not entirely unexpected because it is the conformational flexibility of the benzyl group in **1** that ensures that the dimer configuration eventually fits as neatly as possible into the original reaction cavity, i.e. is responsible for the topotaxy (Thomas 1981). Removal of this group in **2** is in effect the removal of the 'ballast' from the reacting molecule and this in turn is expected to lead to molecular movements during the reaction that are too great to maintain a single-crystal to single-crystal (hence topotactic) reaction. Directional preference for the reaction is an additional question and any rationale for this must follow from the crystal structure, as outlined in the next section.

(*d*) *The crystal structure of lactone* **2**: *occurrence of* C–H···O *hydrogen bonds*

The major interaction between the i.ds is obtained by translating them along [010] to generate a column. When more columns are generated with glide or screw operations, the entire herringbone structure is produced (figure 9). The angle between the molecular plane normal and [010] is 67° and this means that edge-to-edge contacts predominate between i.d. units in the columns. Translation of the i.ds along [010] is expected to reveal the major interaction since the needle axis is *b* and and examination of the short contacts shows that these interactions take the form of C–H···O hydrogen bonds. Figure 10 gives the relevant details for

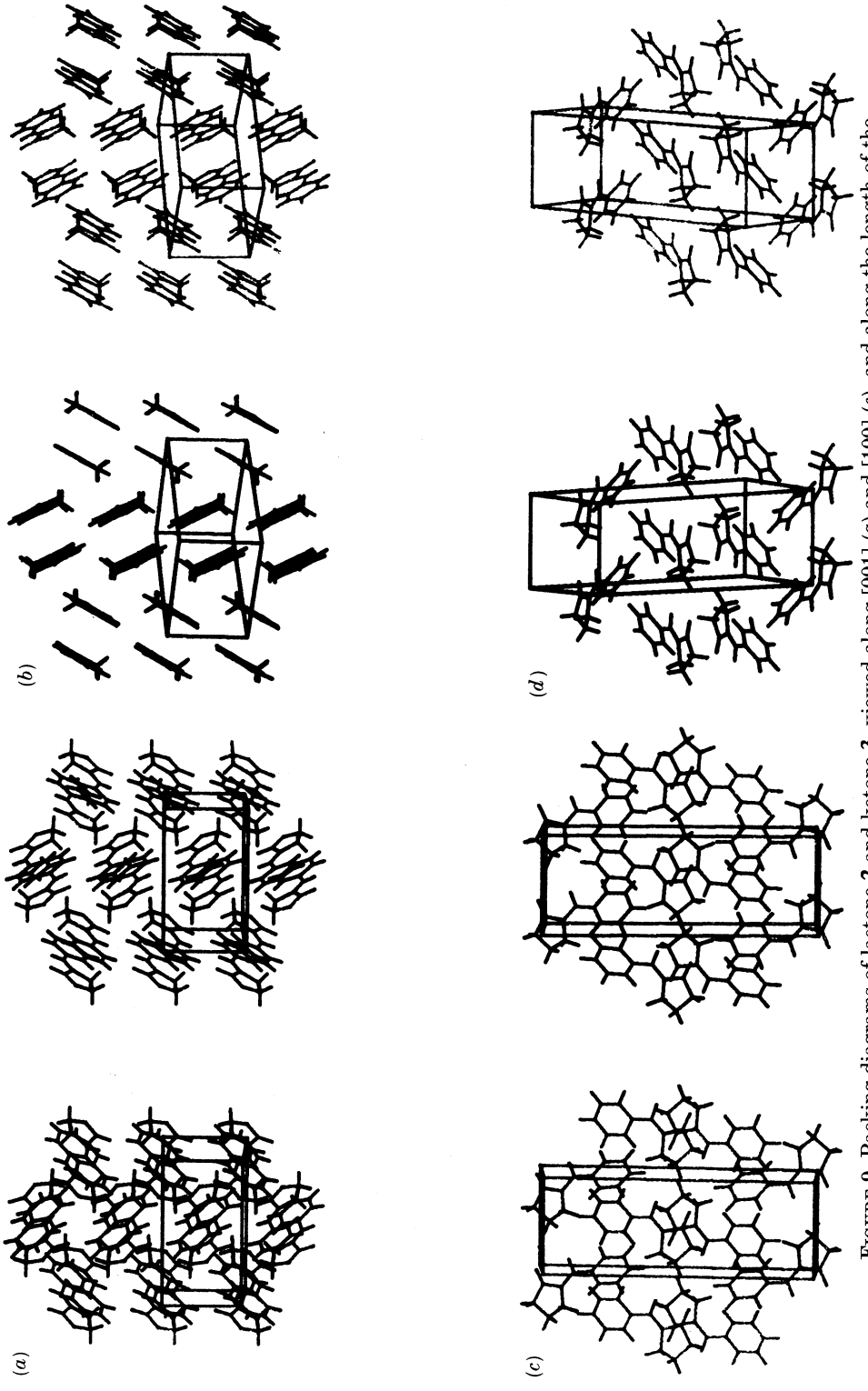

FIGURE 9. Packing diagrams of lactone **2** and ketone **3**, viewed along [001] (*a*) and [100] (*c*), and along the length of the molecule (*b* and *d*) respectively.

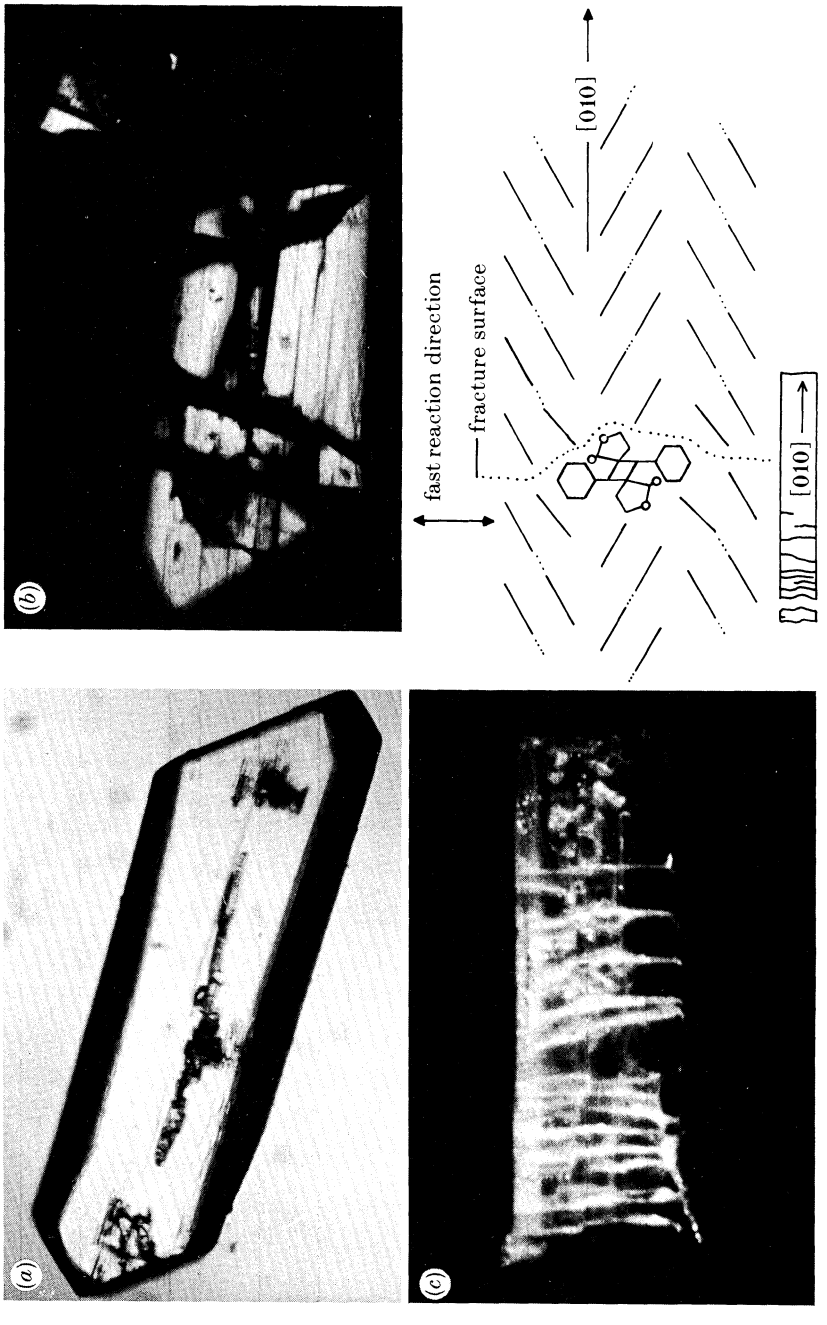

FIGURE 11. Fracture in thick and thin crystals (see text for details).

(*Facing p.* 176)

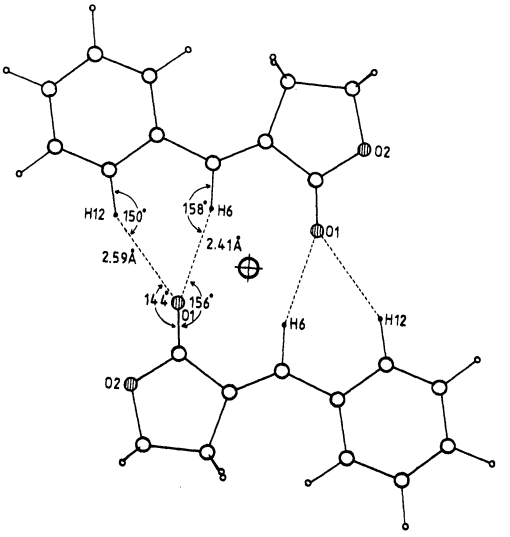

FIGURE 10. Hydrogen bonding scheme between molecules related by inversion (⊕). Hatched atoms are oxygen. The difference in plane levels for the two molecules is approximately 0.5 Å.

the pair of molecules (x, y, z) and $(-x, -1-y, -z)$; all distances and angles are obtained from calculated hydrogen atom positions where the C–H bond vectors have been increased to 1.08 Å. These values become immediately comparable to those given by Taylor & Kennard (1982) in their recent analysis of this phenomenon. According to the geometric criteria they have employed, the intermolecular contacts in the lactone structure, especially those involving aromatic hydrogen atoms, constitute C–H···O hydrogen bonds. Optimization of these interactions is a direct consequence of the planarity of the lactone molecule and it may be suggested that the high density and melting point of this compound follow as a result. Curiously, the lactone oxygen atom O-2 does not participate in such directional C–H···O interactions; this is borne out by a statistical comparison of the occurrence of keto and ether C–H···O hydrogen bonds (Murray–Rust & Glusker 1984). Still, the packing of **2** would seem to indicate that Coulombic forces of this sort certainly play a major role in changing the physical properties of **2** with respect to **3** or even **1**.

We have already seen that the solid state reaction of **2** is not topotactic and reference has been made to crystal fracture perpendicular to [010] while the photoreaction is in progress. It must be emphasized that most organic solid state reactions are not single-crystal to single-crystal. More generally, reactions occur at specific nucleation sites, their progress being accompanied by frontal migration that can be easily monitored (Curtin *et al.* 1979). Such is the case for lactone **2** (figure 11) and there is evidence for a considerable amount of strain being built up in the crystal during reaction; crystals were observed to bend considerably before fracture. For large crystals (at least 0.5 mm in all directions) the strain relief on fracture is manifested as an almost explosive shattering; in several cases, crystal fragments were expelled from below a microscope cover glass! Figure 11 shows a

large crystal (*a*), and fracture at some time after (*b*); (*c*) shows a thinner crystal that fractured less violently, and clearly shows the orientation of the fracture lines. A detailed look at figure 11*b* shows lines of stress parallel to [010], these invariably appear before fracturing and may be explained by some of the strain produced by the reaction being accommodated by splaying of the [010] columnar motifs.

To understand the directional preference for the reaction, it is necessary to refer to figure 9*a* and the schematic explanation on figure 11 where it may be seen that the spread of the reaction would be most rapid along the vector joining double bond centres. This direction is nearly parallel to (010) and means that the reaction is fastest along the densely packed (010) plane and slowest along [010] direction. This is so because, as the reaction proceeds, it will cause the neighbouring i.ds within (010) to be affected first. However, [010] corresponds to the direction of the stabilizing C–H···O contacts and fast reaction in (010) will therefore disrupt these relatively inflexible interactions. These opposing factors create a condition of considerable strain that can only be relieved by violent fracture. This result is almost inevitable because molecule **2** lacks the 'ballast' benzyl group, found in **1**, that is able to compensate for reaction strain by adjusting its own conformation.

(*e*) *Crystal structure of ketone* **3**

If the physical and topochemical properties of **2** can be traced to its planar conformation, the crystal structure of **3** is seen to optimize the packing of a more irregularly shaped non-planar molecule (figure 9*c*).

The important stabilizing interactions in the crystal structure are the edge–plane contacts. Although there is a possibility of C–H···O hydrogen bonds, there is only a suggestion of them when compared to **2**. Figure 12 shows the disposition of four molecules that are related by these interactions. The carbonyl oxygen of the reference molecule (x, y, z; P) has close contacts with H-32 of the translation-related molecule ($x, 1+y, z$; Q) and with H-10 of the screw-related molecule ($1/2-x$, $1/2+y, 1/2-z$; R). At the same time this screw-related molecule is involved in aromatic herringbone edge–ring contacts with the inversion related molecule ($1-x$, $-y$, $-z$; S), with this type of interaction extending into two dimensions. Thus the C–H···O and edge–plane contacts define the geometry of the inversion-related pair. Although the inversion pair (x, y, z; P) and ($1-x$, $-y$, $-z$; S) represent molecules with the anti-parallel carbonyl arrangements, the possible i.d. is defined by the pair (x, y, z) and ($-x$, $-y$, $-z$).

The difference in nonbonding interactions is shown in table 7, which compares short contacts for both structures. The structure of **3** can be described as a more 'typical' organic structure where an irregularly shaped non-planar molecule packs to maximize attractive C···H interactions, unlike lactone **2** that has an unusual structure optimizing C–H···O contacts.

5. Conclusion

Structures that have a pronounced sheetlike character and consist of planar organic molecules (like **2**) pose a challenge to crystallographers, because the presence of one or more very intense *hkl* reflections can create serious problems

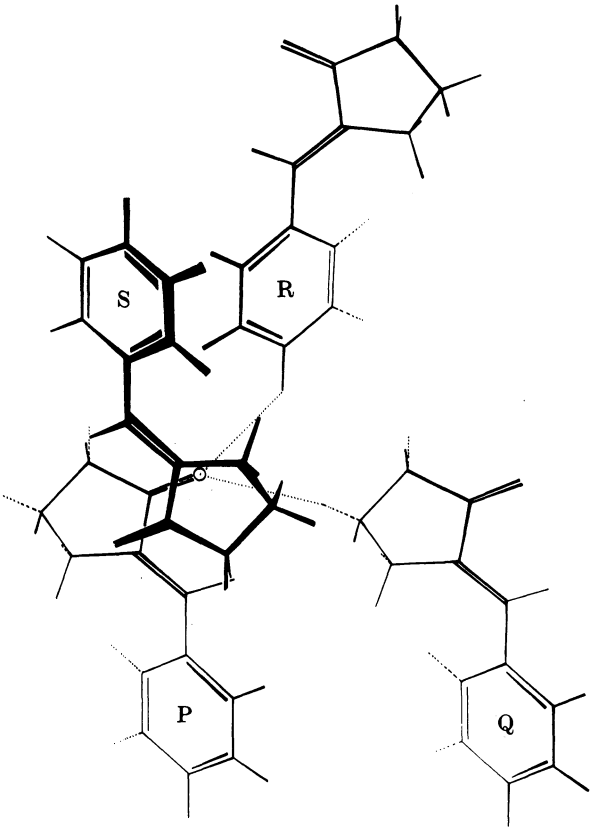

FIGURE 12. Disposition of the four structure-defining molecules for the ketone **3**; see text for details.

TABLE 7. COMPARISON OF THE NUMBER OF SHORT CONTACTS

	C—C		C—H		H—H		O—X		total	
interaction	**2**	**3**	**2**	**3**	**2**	**3**	**2**	**3**	**2**	**3**
ben–ben	6	8	10	26	11	2			27	36
f.m.r.–f.m.r.	3	8	6	6		8	15	23	24	45
ben–f.m.r.	11	4	12	12	8	15	18	4	49	35
total	20	22	28	42	19	25	33	27	100	116

Distances less than the potential minimum for a particular interaction type (see table 4) between benzene (ben) and the five-membered ring (f.m.r.) fragments for both structures. Note how the two fragments for the ketone **3** pack preferentially with themselves, while it is the interaction of these two fragments that is the greatest for the lactone **2**.

in the convergence and phase estimation procedures in programs such as MULTAN 80 and SHELX-76. In this paper we have shown that this difficulty can be circumvented by the use of close packing arguments as outlined by Kitajgorodskij (1965). In general, this would have been a computationally arduous task. However, a knowledge of the solid state reactivity of **2** and a recognition of the principles

of topochemistry, have enabled us to make some helpful simplifying assumptions. For example, we have been able to neglect Coulombic terms even though it has been found they are necessary for a proper description of organic structures. It has been shown here that to some extent the simple dispersive and exchange repulsion potential model can still produce the crystallographically correct structure given some supplemental information and chemical intuition. As the cell is a very strict boundary condition and effectively incorporates all the attractive potential terms, the structure could have been arrived at by considering only the repulsive terms, although the final orientations might have varied slightly. Indeed, during the structure solution it was found more helpful to monitor the repulsive short-range forces.

Accurately calculated lattice energies using nonbonding terms were computed and found to be -83 kJ mol^{-1} for both compounds. This can mean only that one or both structures are not at the minimum with respect to nonbonding forces. To ascertain some of the factors causing the differences in the physical properties it will be necessary to look at intramolecular, static and dynamic–intermolecular forces in more detail.

The authors thank Professor J. M. Thomas, F.R.S., for the keen interest and enthusiasm that he has shown in this work. We appreciate the encouragement of Dr S. Ramdas. We thank Dr W. Jones and Dr C. R. Theocharis for arranging to collect the X-ray data for the compounds studied. This work was largely carried out while G.R.D. was a summer visitor at the Department of Physical Chemistry, University of Cambridge. S.K.K. acknowledges the support of S.E.R.C. for a studentship. Full details of the procedures adopted in the computation of the contour maps may be found in the Ph.D. thesis of S.K.K. submitted to the University of Cambridge, 1983.

References

Adams, J. M. & Ramdas, S. 1979 *Acta crystallogr.* B **35**, 679–683.
Birkofer, L. & Barnikel, C.-D. 1958 *Chem. Ber.*, **91**, 1996–1999.
Birkofer, L., Kim, S. & Engels, M. D. 1962 *Chem. Ber.* **95**, 1495–1504.
Cohen, M. D. & Schmidt, G. M. J. 1964 *J. chem. Soc.*, 1996–2000.
Cox, S. R., Hsu, L.-Y. & Williams, D. E. 1981 *Acta crystallogr.* A **37**, 293–301.
Curtin, D. Y., Paul, I. C., Duesler, E. N., Lewis, T. W., Mann, B. J. & Shiau, W.-L. 1979 *Molec. Cryst. Liq. Cryst.* **50**, 25.
Desiraju, G. R., Kamala, R., Kumari, B. H. & Sarma, J. A. R. P. 1984 *J. chem. Soc. Perkin Trans.* II, 181–189.
Drenth, W. & Wiebenga, E. H. 1955 *Acta crystallogr.* **8**, 755–760.
Eiermann, R., Parkinson, G. M., Bassler, H. & Thomas, J. M. 1983 *J. phys. Chem.* **87**, 544–551.
Frank, J. K. & Paul, I. C. 1973 *J. Am. chem. Soc.* **95**, 2324–2332.
Germain, G., Main, P. & Woolfson, M. M. 1971 *Acta crystallogr.* A **27**, 368.
Gougoutas, J. Z. 1971 *Pure appl. Chem.* **27**, 305.
Gougoutas, J. Z. 1975 *J. solid St. Chem.*, **12**, 51.
Gramaccioli, C. M., Filippini, G., Simonetta, M., Ramdas, S., Parkinson, G. M. & Thomas, J. M. 1980 *J. chem. Soc. Faraday Trans.* II **76**, 1336–1346.
Jones, W., Ramdas, S. & Thomas, J. M. 1978 *Chem. Phys. Lett.* **54**, 490–493.
Jones, W., Nakanishi, H., Theocharis, C. R. & Thomas, J. M. 1980 *Chem. Soc. chem. Commun.*, 610.
Kaupp, G. & Zimmermann I. 1981 *Angew. Chem. int. Edn. Engl.*, **20**, 1018.

Kaupp, G., Jostkleigrewe, E. & Hermann, H.-J. 1982 *Angew. Chem. int. Edn. Engl.*, **21**, 435.
Kearsley, S. K. 1983 Ph.D. thesis, University of Cambridge.
Kitajgorodskij, A. I. 1965 *Acta crystallogr.* **18**, 585–590.
Momany, F. A., Carruthers, L. M., McGuire, R. F. & Scheraga, H. A. 1974 *J. phys. Chem.* **78**, 1595–1620.
Murray-Rust, P. & Glusker, J. P. 1984 *J. Am. chem. Soc.* **106**, 1018–1025.
Nakanishi, H., Jones, W., Thomas, J. M., Hasegawa, M. & Rees, W. L. 1980 *Proc. R. Soc. Lond.* A **369**, 307–325.
Nakanishi, H., Jones, W., Thomas, J. M., Hursthouse, M. B. & Motevalli, M. 1981 *J. phys. Chem.* **85**, 3636–3642.
Paul, I. C. & Curtin, D. Y. 1973 *Acct. chem. Res.* **7**, 223.
Reppe, W. 1955 *Annln Chem.* **596**, 158(183).
Ramdas, S., Thomas, J. M. & Goringe, M. J. 1977 *J. chem. Soc. Faraday Trans.* II **76**, 551–561.
Ramdas, S. 1979 *Chem. phys. Lett.* **60**, 320–322.
Ramdas, S., Thomas, J. M., Jordan, M. E. & Eckhardt, C. J. 1981 *J. phys. Chem.* **85**, 2421–2425.
Schmidt, G. M. J. 1971 *Pure appl. Chem.* **27**, 647–679.
Sheldrick, G. M. 1976 SHELX-76, *Programme for crystal structure determination*. University of Cambridge, England.
Taylor, R. & Kennard, O. 1982 *J. Am. chem. Soc.* **104**, 5063–5070.
Theocharis, C. R., Jones, W., Thomas, J. M., Hursthouse, M. B. & Motevalli, M. 1984 *J. chem. Soc. Perkin Trans.* II, 71–76.
Thomas, J. M. 1974 *Phil. Trans. R. Soc. Lond.* A **277**, 251.
Thomas, J. M., Morsi, S. E. & Desvergne, J.-P. 1977 *Adv. phys. Chem.* **15**, 63.
Thomas, J. M. 1981 *Nature, Lond.* **289**, 633.
Wegner, G. 1969 *Z. Naturf.* **24**b, 824.
Wegner, G. 1971 *Makromolec. Chem.* **145**, 85.
Williams, D. E. 1969 *Acta crystallogr.* A **25**, 464.
Williams, D. E. 1971 *Acta crystallogr.* A **27**, 452–455.
Williams, D. E. 1972 *Acta crystallogr.* A **28**, 629–635.
Williams, D. E. & Starr, T. L. 1977 *Computers Chem.* **1**, 173–177.

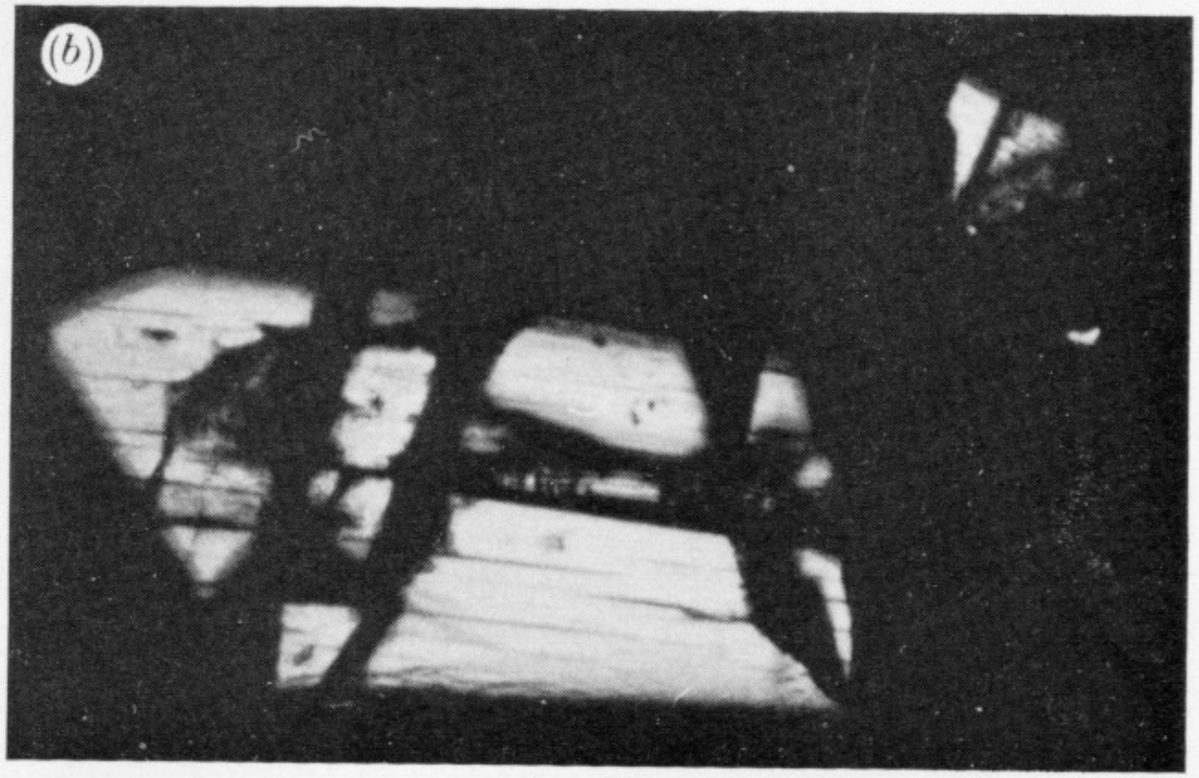

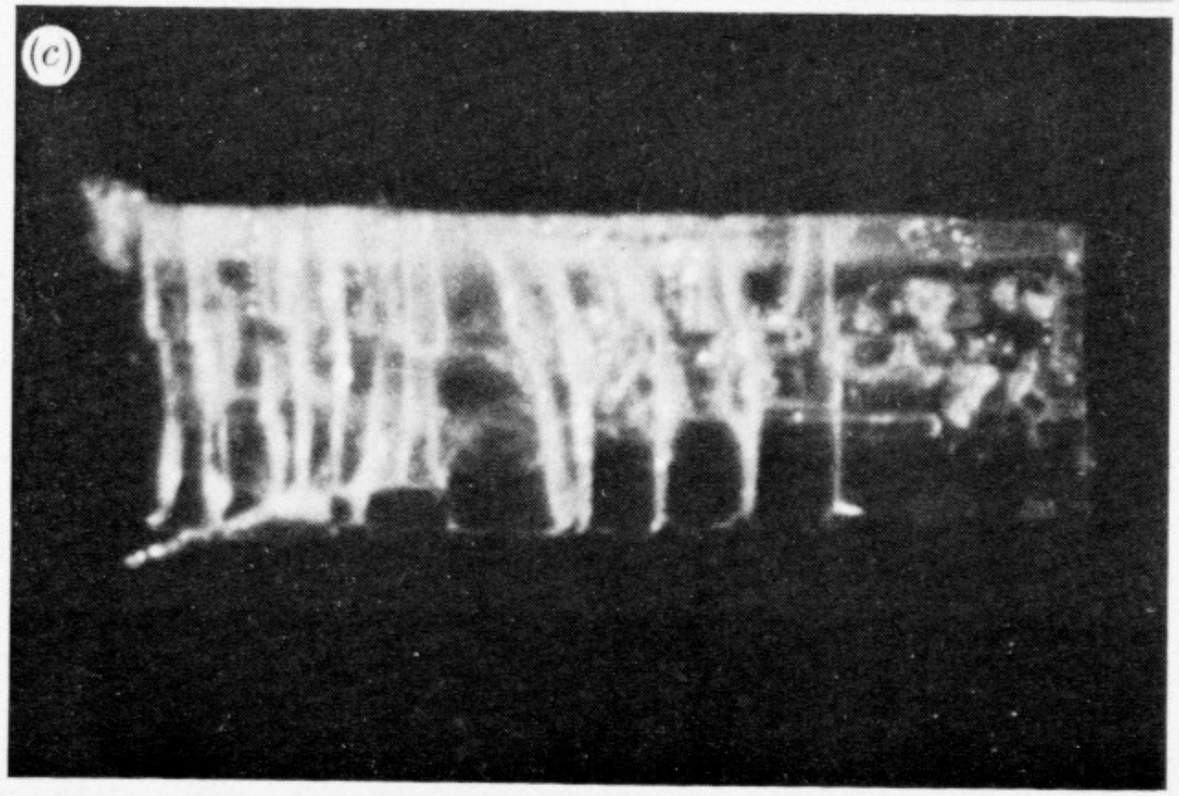

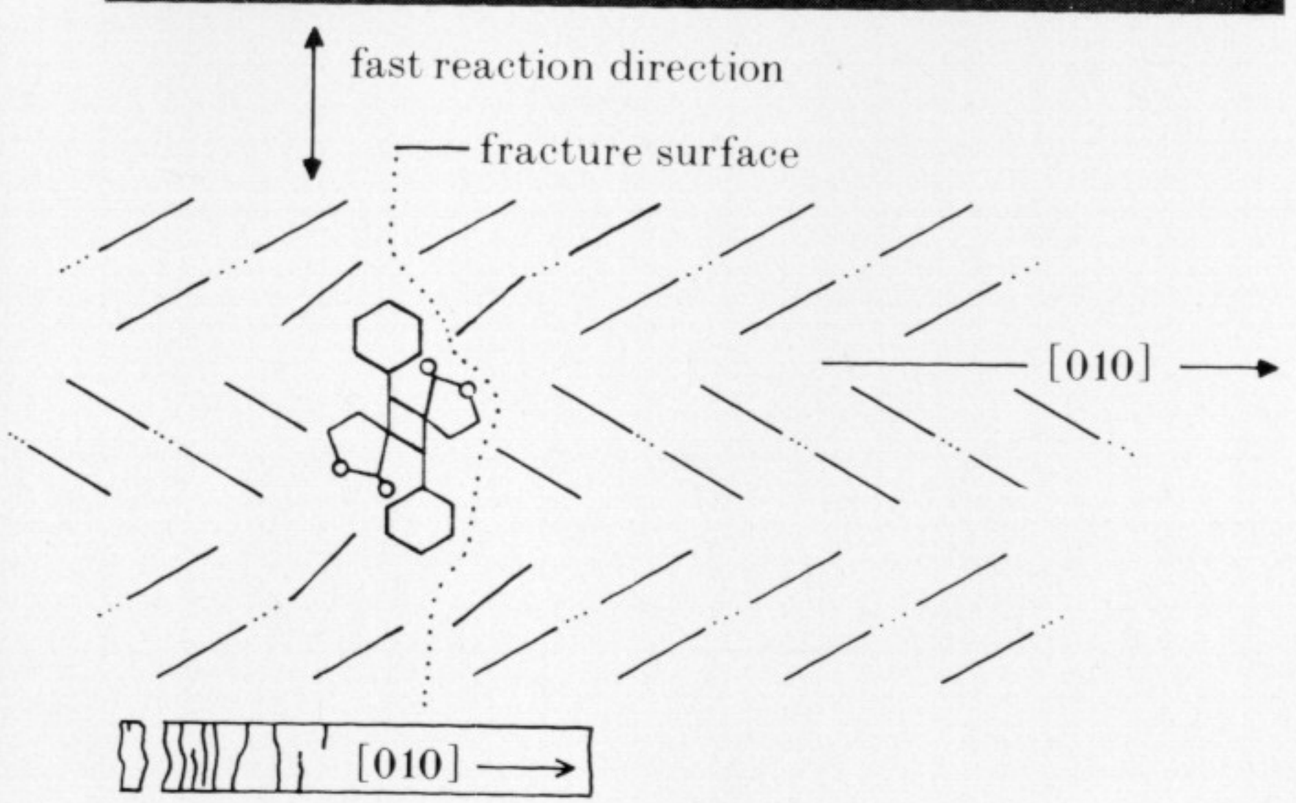

FIGURE 11. Fracture in thick and thin crystals (see text for details).